

# Molecular Junctions: Can Pulling Influence Optical Controllability?

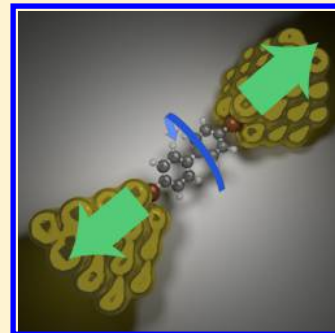
Shane M. Parker,<sup>†</sup> Manuel Smeu,<sup>†</sup> Ignacio Franco,<sup>‡</sup> Mark A. Ratner,<sup>†</sup> and Tamar Seideman<sup>\*,†</sup>

<sup>†</sup>Department of Chemistry, Northwestern University, Evanston, Illinois 60208, United States

<sup>‡</sup>Department of Chemistry, University of Rochester, Rochester, New York 14627, United States

**S** Supporting Information

**ABSTRACT:** We suggest the combination of single molecule pulling and optical control as a way to enhance control over the electron transport characteristics of a molecular junction. We demonstrate using a model junction consisting of biphenyl-dithiol coupled to gold contacts. The junction is pulled while optically manipulating the dihedral angle between the two rings. Quantum dynamics simulations show that molecular pulling enhances the degree of control over the dihedral angle and hence over the transport properties.



**KEYWORDS:** Optical control, molecular junction, single-molecule pulling, electron transport, molecular conductance

The field of molecular electronics has seen rapid progress in recent years, motivated both by the exciting challenges in fundamental chemical physics and by the potential for impactful technological applications.<sup>1</sup> Over the last decades, powerful experimental<sup>2–4</sup> and computational<sup>5,6</sup> techniques have been developed to characterize and understand the properties of single-molecule junctions.

More recently, the topic of control in a junction has been explored. The most common control motifs are optical and mechanical but control by chemical<sup>7,8</sup> and electrical<sup>9,10</sup> means has also been investigated. In general, the combination of optical fields and molecular electronics comprises molecular optoelectronics.<sup>11</sup> Perhaps the simplest route to optical control of a molecular junction is with switching. One approach to switching is to induce a (preferably reversible) conformational change between metastable molecular states with different conductivities, for example, by photoisomerizing<sup>12,13</sup> or by aligning surface-adsorbed molecules in a moderately intense laser field.<sup>14,15</sup> Control has also been realized more directly by, for example, using low-frequency off-resonant radiation to modulate energy levels (these are termed adiabatic processes)<sup>16,17</sup> with a strong few-cycle laser pulse<sup>18</sup> or with near-resonant radiation that electronically excites the junction (either the molecule<sup>19</sup> or electrodes<sup>20</sup>).

The first demonstration of mechanical control in a molecular junction was the amplification of the current of a single fullerene (C<sub>60</sub>) by pressing on the molecule with a metallic tip.<sup>21</sup> A mechanically activated switch was proposed in ref 22, where a conductive AFM tip was used to toggle between folded and unfolded states of a  $\pi$ -stacking molecule. The conductance of conjugated polymers,<sup>23</sup> alkanedithiols,<sup>24</sup> and DNA<sup>25</sup> under mechanical stress have also been reported.

In this Letter, we consider combining optical and mechanical control in a junction. Several strategies have been reported previously in which light absorption is used to alter the mechanical response of a molecule.<sup>26,27</sup> In what follows, we describe the converse; a mechanical force is used to enhance a molecule's susceptibility for optical control.

We use biphenyl-dithiol (see Figure 1) as a model to demonstrate the possibility of using optical control during a

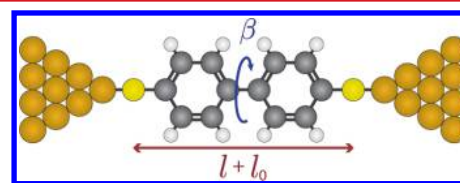


**Figure 1.** Biphenyl-dithiol junction showing the torsion angle between the two rings,  $\beta$ , and the sulfur–sulfur distance,  $l + l_0$ , with  $l_0$  the equilibrium distance. Gold contacts were included explicitly in transport calculations. Sulfurs were terminated with hydrogen atoms for potential energy surface calculations.

molecular pulling experiment.<sup>28</sup> The torsion angle between the two rings in biphenyl determines the degree of electronic coupling between the rings, thus influencing absorption and emission spectra<sup>29</sup> and electron transfer and transport rates.<sup>7,8,30</sup> Closer to coplanar configurations are expected to have reduced absorption energies and enhanced transfer and transport rates.

**Received:** May 1, 2014

**Revised:** July 17, 2014

**Published:** July 29, 2014

The torsion angle can be controlled optically with a nonresonant circularly or elliptically polarized laser pulse, as suggested in the theoretical work of ref 31 and shown in the experimental works of refs 32 and 33. For a more general discussion of control with nonresonant fields, see ref 34. Here, the laser propagation direction should be perpendicular to the inter-ring axis. In the nonresonant regime, the rings are pushed toward the coplanar configuration by the interaction between the electric field and the induced-dipole of each ring. The degree of coplanarity that can be achieved optically (and thus the degree of control that can be imposed on conductance) depends on the interaction strength  $\Omega = (1/8)E^2\Delta\alpha$ , where  $E$  is the electric field and  $\Delta\alpha$  is the polarizability anisotropy, and the barrier to coplanarity,  $V_{\parallel}$ . The higher the barrier to coplanarity, the larger  $\Omega$  needs to be for controllability. Conversely, the controllability could be enhanced by lowering  $V_{\parallel}$ .

The existence of such a barrier to coplanarity can be viewed as the result of a competition between inter-ring resonance (favoring the coplanar configuration) and steric hindrance (favoring the perpendicular configuration). Naïvely, one could expect to mitigate the steric hindrance by pulling along the inter-ring axis so as to increase the separation between ortho hydrogen pairs. The effect of this would be to reduce the barrier to coplanarity, thereby enhancing the degree of coplanarity achievable optically.

The remainder of this article further explores this idea by investigating the roles that molecular pulling and torsion play in the optical control and single-molecule conductance of biphenyl-dithiol. A depiction of our molecular junction is given in Figure 1.

While the effects of torsion and pulling are individually well studied, the effect of the combined stimulus on the molecular conductance is less clear. It has been shown both computationally<sup>30</sup> and experimentally<sup>7,8</sup> that molecular conductance increases as biphenyl planarizes. On the other hand, molecular conductance generally tends to decrease with elongation.<sup>23,35,36</sup> To investigate how the concerted application of these stimuli affects the conductance properties of biphenyl-dithiol in a junction, we carried out electron transport calculations for strained junctions using the nonequilibrium Green's function formalism within density functional theory (NEGF-DFT).<sup>5,37</sup> Details of the computations and the computed transmission functions for the junction are included in Section III of the Supporting Information. Figure 2 shows the resulting zero-bias

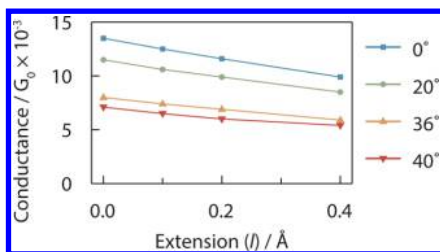


**Figure 2.** Conductance as a function of extension,  $l$ , for various torsional angles.

conductance for the junction as a function of molecular elongation for different fixed torsional angles. While stretching the molecule does decrease its conductance, the structural parameter that clearly dominates the conductance is the torsion. Thus, we focus on the molecule's planarity as a means to control the conductance.

The effect that pulling exerts on the optical controllability of the degree of coplanarity was examined using quantum dynamics simulations of the torsional control of biphenyl-dithiol. These simulations use a circularly polarized laser pulse of varying duration at different fixed pulling distances. We focus on the one-dimensional torsion dynamics at finite temperature. Although this ignores coupling between the torsion coordinate and the combined rotation of both rings, such one-dimensional model dynamics have exhibited excellent agreement with nonadiabatic two-dimensional rotational–torsional dynamics measured experimentally in prealigned biphenyl derivatives.<sup>38</sup> Similarly, simulations of control in the adiabatic limit of a freely rotating biphenyl molecule (i.e., not prealigned) have shown qualitatively similar control as the one-dimensional prealigned problem, although it was suggested that higher intensities may be needed to overcome coupling between the overall rotations and torsion (which are anyways absent in the prealigned case).<sup>39</sup> The density matrix,  $\rho$ , is propagated in time according to

$$\dot{\rho} = -i[\mathcal{H}_F, \rho] \quad (1)$$

where  $\mathcal{H}_F = \mathcal{H}_F^0 + \mathcal{V}_F^{\text{int}}(t)$  is the Hamiltonian operator,  $\mathcal{H}_F^0$  is the field-free Hamiltonian, and  $\mathcal{V}_F^{\text{int}}(t)$  describes the interaction with the field ( $\hbar = 1$ ). The subscript F indicates force-dependence. In this model, the field-free molecular torsional Hamiltonian is given by

$$\mathcal{H}_F^0 = -\frac{1}{2I_F} \frac{\partial^2}{\partial \beta^2} + \mathcal{V}_F^{\text{tors}} \quad (2)$$

where  $I_F$  is the moment of inertia of the relative torsional coordinate  $\beta$ , and  $\mathcal{V}_F^{\text{tors}}$  is the torsional potential. Likewise, the interaction between the field and the induced-dipole takes the form<sup>31,40</sup>

$$\mathcal{V}_F^{\text{int}}(t) = -\frac{1}{8} |\Delta\alpha_F| \cos^2 \beta E_r^2(t) \quad (3)$$

where  $E_r(t)$  is the Gaussian envelope function of the circularly polarized field with full width at half-maximum of  $\tau$  and  $|\Delta\alpha_F|$  is the force-dependent polarizability anisotropy. The tip–surface junction that motivates this model would exhibit a plasmonic enhancement of the incident electric field of about 1 order of magnitude;<sup>15</sup> however, here we consider only the effective field intensity, that is, the field that the molecule experiences after being enhanced by plasmonic or other mechanisms. Finally, the density matrix is expanded in the eigenbasis of the field-free Hamiltonian and is then propagated numerically from a thermal initial state.

Computation of the quantum dynamics for a given pulling force requires knowledge of the force-dependence of the torsion potential energy surface, the polarizability anisotropy, and the moment of inertia. These are determined by first computing a partially relaxed potential energy surface of (hydrogen terminated) biphenyl-dithiol on a two-dimensional grid as a function of the extension,  $l$ , and the torsional coordinate,  $\beta$ , both specified in Figure 1. All constrained geometry optimizations were performed using the M06-2X density functional<sup>41</sup> with the def2-TZVP basis set,<sup>42</sup> as implemented in the Q-Chem package.<sup>43</sup> We then fit the surface to a Hill-equation of the form

$$\mathcal{V}(l, \beta) = V_0(l) + \sum_{n=1}^N V_{2n}(l) \cos(2n\beta) \quad (4)$$

where the  $V_{2n}(l)$  are polynomial fits of the Fourier coefficients of the torsional potential at each extension and  $N = 4$ . A comparison of the computed Fourier coefficients and the polynomial fits is shown in Figure S1 of the Supporting Information. Importantly, we indeed find that pulling on the molecule (increasing the sulfur–sulfur distance) decreases the barrier to coplanarity. This effect is demonstrated in Figure 3,

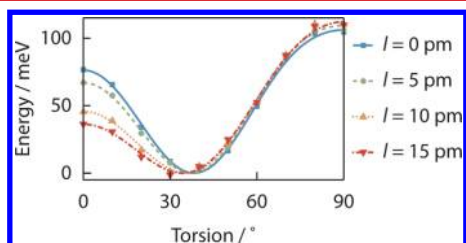


**Figure 3.** Slices of the potential energy surface at different pulling distances showing the computed torsional potential (marks) and the potential fit to a four-term Fourier expansion (lines) as in eq 4. The zero of energy is defined as the minimum of the torsional potential energy surface at each pulling distance.

where a few slices of the computed potential energy surfaces and their corresponding fits are shown. The force required to hold the molecule at a given extension, averaged over the torsional coordinate, is shown in Figure 4 and given by

$$F_0(l) = \frac{\partial V_0(l)}{\partial l} \quad (5)$$

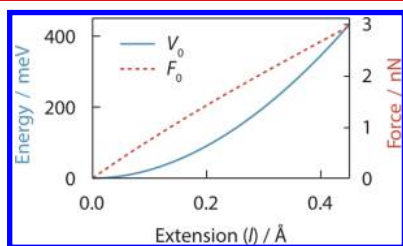


**Figure 4.** Static Fourier component of the potential energy surface,  $V_0$  (defined in eq 4), and the mean force required to hold the molecule at a particular distance,  $F_0$  (defined in eq 5).

For simplicity, we require the moment of inertia to be constant with respect to the torsion angle. For each extension distance, the moment of inertia about the inter-ring axis is averaged over the torsional coordinate and this average moment of inertia is fit to a polynomial form (see Figure S2 of the Supporting Information). Similarly, we determined  $\Delta\alpha_F$  by computing the static polarizability and the dynamic polarizability (at a wavelength of 800 nm) at each extension. Polarizabilities were calculated using TD-HF and the def2-TZVP basis set in Q-Chem. Finally, the resulting polarizability anisotropies from each extension were fit to a linear form (see Figure S2 of the Supporting Information). Because the computed static and dynamic polarizabilities differed by less than 1%, we proceed with only the static polarizabilities.

A convenient metric for the degree of coplanarity (and hence for the conductance) is the expectation value  $\langle \cos^2 \beta \rangle$ , which ranges from 0 in the fully perpendicular configuration to 1 in

the fully coplanar configuration. We investigated the combined influence of field intensity and pulling force on the maximum achieved  $\langle \cos^2 \beta \rangle$  with two different pulse shapes and at two different temperatures. Pulse shapes can be classified into two extreme regimes: the adiabatic in which the pulse width is much longer than the torsional period, and the nonadiabatic or sudden, in which the opposite holds, that is, the pulse width is short compared to the torsional period. The two regimes differ mainly in the time scale over which control is retained. For adiabatic pulses, maximum coplanarity is retained for as long as the field is applied. On the other hand, the nonadiabatic pulse initiates coherent torsional motion and the maximal torsional alignment is attained transiently at multiples of the torsional period. The period of torsion in our model system is force-dependent but on the order of 1 ps. For a more detailed discussion of the effect of pulse shapes we refer the reader to refs 44 and 45 in the context of molecular alignment and ref 46 in the context of torsion in biaryl compounds. The results from two sets of simulations, one adiabatic (with  $\tau = 50$  ps) and one nonadiabatic (with  $\tau = 0.5$  ps), are shown in Figure 5. Both sets

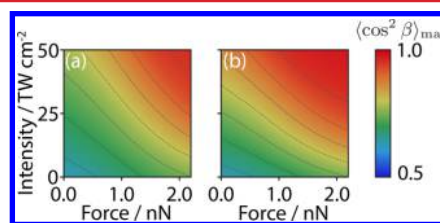


**Figure 5.** Maximum achieved  $\langle \cos^2 \beta \rangle$  as a function of pulling force and field intensity for an ensemble with initial temperature 50 K and a pulse with (a)  $\tau = 50$  ps and (b)  $\tau = 0.5$  ps.

used an initial temperature of 50 K. Although the pulse shape indeed alters the achieved  $\langle \cos^2 \beta \rangle$ , the qualitative features are consistent in both regimes: the degree of coplanarity achievable using both a pulling force and an optical field is much greater than the degree of coplanarity achievable by either of them alone. We also repeated the above dynamics calculations at an elevated temperature of 150 K and found that while an increased temperature decreases the degree of control that can be realized, it does not alter the qualitative behavior we have just described. The results of these simulations are presented in Figure S3 of the Supporting Information.

We can quantify the efficacy of this approach by asking how one can get the most “bang for the buck”: What is the greatest degree of coplanarity that can be achieved subject to particular constraints on the optical field and pulling force? These constraints could be related to, for example, the experimental realizability of a given control pulse or the stability of the molecule or junction subject to an intense laser field and a strong pulling force.

We explore this concept by defining a unitless generic cost function,

$$\mathcal{J}_{I,F}^k(I, F) = \left| \frac{I}{J_I} \right|^k + \left| \frac{F}{J_F} \right|^k \quad (6)$$

where  $I$  and  $F$  are the maximum field intensity and pulling force of a given simulation and  $J_I$  and  $J_F$  are free parameters that define the relative cost of the optical field and the pulling force. A cost function is specified by choosing the order of the cost,  $k$ , and by choosing values of the intensity and the pulling force

that are “comparable.” For any set of simulations with the same pulse shape and temperature, finding the maximum values of achieved  $\langle \cos^2 \beta \rangle$  along successive isocontours of the cost function forms a minimum cost path. This is the path one would follow in order to increase the achieved coplanarity in the most cost-effective way with the given pulse shape and temperature.

A “true” cost function representing the stress on a junction (if one exists) would be an extremely complex, highly nonlinear function of not only field intensity and pulling force but also laser frequency, pulse duration and shape, molecular orientation, temperature, pressure, environment, anchoring groups, the junction material, and so forth. Our cost function does not attempt to capture this complexity; it is primarily an illustrative tool.

Because a particular minimum cost path is determined by the ratio of  $J_I$  and  $J_F$ , we define the parameter

$$\Lambda = \left( \frac{J_I}{50 \text{ TW cm}^{-2}} \right) \left( \frac{J_F}{2.0 \text{ nN}} \right) \quad (7)$$

and examine values of  $\Lambda$  from 1/3 to 3. This (more than) covers a range of 25–75 TW/cm<sup>2</sup> for  $J_I$  and a range of 1.0–2.5 nN for  $J_F$ , which correspond to the range of saturation ionization intensities found for several benzene derivatives<sup>47,48</sup> and to rupture forces of common molecular anchoring groups,<sup>49</sup> respectively. With this, the saturation ionization intensity and bond rupture forces have the same cost associated with them, that is, the points at which each stimulus destroys the molecule are considered comparable. Some minimum cost paths associated with linear and quadratic cost functions (eq 6 with  $k = 1$  and  $k = 2$ , respectively) are shown in Figure 6. For

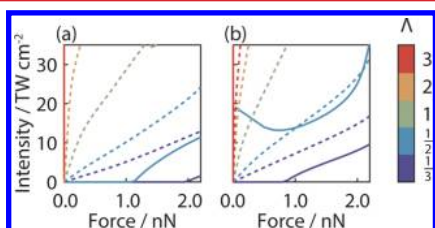


**Figure 6.** Linear (solid) and quadratic (dashed) minimum cost paths for pulses with (a)  $\tau = 50$  ps and (b)  $\tau = 0.5$  ps. The initial temperature in all cases was 50 K. See eq 7 for a definition of  $\Lambda$ . In total, five values of  $\Lambda$  are plotted from  $\Lambda = 1/3$  (blue) to  $\Lambda = 3$  (red).

both the adiabatic and nonadiabatic pulses, minimum cost paths of quadratic cost functions strongly combine pulling and field intensity. By contrast, only certain values of  $\Lambda$  result in minimum cost paths that effectively combine the two when a linear cost function is used. One would expect higher order costs (larger  $k$ ) to more strongly favor the combination. This indicates that for the class of cost functions employed here, there exist values of  $\Lambda$  for which one should simultaneously employ optical and mechanical forces if one wants the most bang for one’s buck. See Figure S4 of the Supporting Information for the corresponding minimum cost paths at 150 K.

In summary, we have described a scenario in which a molecule’s susceptibility to optical control could be enhanced in the context of a single molecule pulling experiment and have shown that such control could effectively modulate the molecular conductance. The enhanced controllability was demonstrated numerically with quantum dynamics simulations

of a simple 1D model of torsion in biphenyl-dithiol. The qualitative effect is robust with respect to pulse shape and ensemble temperature, even if the quantitative results depend on such properties strongly. Although we focused on biphenyl-dithiol as a model, we note that this same strategy could be applied to any biaryl compound with a twisted equilibrium configuration resulting from a competition between aromaticity and steric hindrance. Therefore, the intensities employed here could be reduced by choosing a molecule with a larger polarizability anisotropy or a lower barrier to torsion. Our cost analysis revealed that the benefit to combining pulling and optical control depends on the order of the cost involved, but for each class of cost functions considered, there exist situations in which the most cost-effective path utilized this kind of mixed control. NEGF-DFT electron transport calculations demonstrate that the influence of torsion on conductance is much greater than the influence of molecular pulling, thus preserving the ability of such a junction to act as a torsional switch.

While capturing all possible effects that could in principle play a role during an optomechanical experiment is beyond present-day computational capabilities, the robustness of the cost analysis above suggests that the benefits of coupling pulling and laser control will survive even in the presence of added complications. Experimental input is thus crucial to make further progress and clarify the effect that laser-induced excitations in the leads may have on the transport and mechanical response of the junction.

This strategy should prove interesting in molecular junctions, especially light driven junctions.<sup>11</sup> With biphenyl as an example, one could envision applying a small force in the junction to modulate the current directly (by decreasing the torsion angle and thus increasing the inter-ring coupling) and indirectly (by enhancing the molecule’s optical response). Furthermore, exercising this type of control in statistical junction experiments could reduce the extent of experiment-to-experiment fluctuations, resulting in sharper conductance histograms.<sup>50</sup>

## ■ ASSOCIATED CONTENT

### Supporting Information

Details on the fits of the polarizability anisotropy and moment of inertia (Figures S1 and S2), the quantum dynamics results at 150 K (Figures S3 and S4), and the details of the molecular conductance calculations (Figures S5–S8). This material is available free of charge via the Internet at <http://pubs.acs.org>.

## ■ AUTHOR INFORMATION

### Corresponding Author

\*E-mail: [t-seideman@northwestern.edu](mailto:t-seideman@northwestern.edu).

### Notes

The authors declare no competing financial interest.

## ■ ACKNOWLEDGMENTS

S.M.P. thanks the Department of Energy for a Graduate Fellowship. M.S. thanks the FRQNT for financial support. M.A.R. thanks the Chemistry Division of the National Science Foundation for support (Grant CHE-1058896). T.S. thanks the National Science Foundation (Grant CHE-1012207) and the Department of Energy (Grant DE-SC0001785).

## ■ REFERENCES

- (1) Cuevas, J. C.; Scheer, E. *Molecular Electronics: An Introduction to Theory and Experiment*; World Scientific series in nanoscience and nanotechnology; World Scientific: Hackensack, 2010.
- (2) Li, C.; Mishchenko, A.; Wandlowski, T. *Top. Curr. Chem.* **2012**, *313*, 121–188.
- (3) Tao, N. J. *Nat. Nanotechnol.* **2006**, *1*, 173–181.
- (4) Arroyo, C. R.; Tarkuc, S.; Frisenda, R.; Seldenthuis, J. S.; Woerde, C. H. M.; Eelkema, R.; Grozema, F. C.; van der Zant, H. S. J. *Angew. Chem., Int. Ed.* **2013**, *125*, 3234–3237.
- (5) Taylor, J.; Guo, H.; Wang, J. *Phys. Rev. B* **2001**, *63*, 245407.
- (6) Xue, Y.; Datta, S.; Ratner, M. A. *Chem. Phys.* **2002**, *281*, 151–170.
- (7) Mishchenko, A.; Vonlanthen, D.; Meded, V.; Bürkle, M.; Li, C.; Pobelov, I. V.; Bagrets, A.; Viljas, J. K.; Pauly, F.; Evers, F.; Mayor, M.; Wandlowski, T. *Nano Lett.* **2010**, *10*, 156–163.
- (8) Vonlanthen, D.; Mishchenko, A.; Elbing, M.; Neuburger, M.; Wandlowski, T.; Mayor, M. *Angew. Chem., Int. Ed.* **2009**, *48*, 8886–8890.
- (9) Cacelli, I.; Ferretti, A.; Girlanda, M.; Macucci, M. *Chem. Phys.* **2006**, *320*, 84–94.
- (10) Seldenthuis, J. S.; Prins, F.; Thijssen, J. M.; van der Zant, H. S. J. *ACS Nano* **2010**, *4*, 6681–6686.
- (11) Galperin, M.; Nitzan, A. *Phys. Chem. Chem. Phys.* **2012**, *14*, 9421–9438.
- (12) Dulić, D.; van der Molen, S. J.; Kudernac, T.; Jonkman, H. T.; de Jong, J. J. D.; Bowden, T. N.; van Esch, J.; Feringa, B. L.; van Wees, B. J. *Phys. Rev. Lett.* **2003**, *91*, 207402.
- (13) He, J.; Chen, F.; Liddell, P. A.; Andréasson, J.; Straight, S. D.; Gust, D.; Moore, T. A.; Moore, A. L.; Li, J.; Sankey, O. F.; Lindsay, S. M. *Nanotechnology* **2005**, *16*, 695–702.
- (14) Reuter, M. G.; Sukharev, M.; Seideman, T. *Phys. Rev. Lett.* **2008**, *101*, 208303.
- (15) Reuter, M. G.; Ratner, M. A.; Seideman, T. *Phys. Rev. A* **2012**, *86*, 013426.
- (16) Tien, P. K.; Gordon, J. P. *Phys. Rev.* **1963**, *129*, 647–651.
- (17) Franco, I.; Shapiro, M.; Brumer, P. *Phys. Rev. Lett.* **2007**, *99*, 126802.
- (18) Schiffrin, A.; et al. *Nature* **2013**, *493*, 70–74.
- (19) Yasutomi, S.; Morita, T.; Imanishi, Y.; Kimura, S. *Science* **2004**, *304*, 1944–1947.
- (20) Wang, L.; May, V. J. *Phys. Chem. C* **2010**, *114*, 4179–4185.
- (21) Joachim, C.; Gimzewski, J. K. *Chem. Phys. Lett.* **1997**, *265*, 353–357.
- (22) Franco, I.; Solomon, G. C.; Schatz, G. C.; Ratner, M. A. *J. Am. Chem. Soc.* **2011**, *133*, 15714–15720.
- (23) Lafferentz, L.; Ample, F.; Yu, H.; Hecht, S.; Joachim, C.; Grill, L. *Science* **2009**, *323*, 1193–1197.
- (24) Li, Y.; Yin, Z.; Yao, J.; Zhao, J. *Chem. Lett.* **2009**, *38*, 334–335.
- (25) Chang, S.; He, J.; Kibel, A.; Lee, M.; Sankey, O.; Zhang, P.; Lindsay, S. *Nat. Nanotechnol.* **2009**, *4*, 297–301.
- (26) Hugel, T. *Science* **2002**, *296*, 1103–1106.
- (27) McCullagh, M.; Franco, I.; Ratner, M. A.; Schatz, G. C. *J. Am. Chem. Soc.* **2011**, *133*, 3452–3459.
- (28) Franco, I.; Schatz, G. C.; Ratner, M. A. *J. Chem. Phys.* **2009**, *131*, 124902.
- (29) Beenken, W. J. D.; Lischka, H. J. *Chem. Phys.* **2005**, *123*, 144311.
- (30) Solomon, G. C.; Andrews, D. Q.; Van Duyne, R. P.; Ratner, M. A. *ChemPhysChem* **2009**, *10*, 257–264.
- (31) Ramakrishna, S.; Seideman, T. *Phys. Rev. Lett.* **2007**, *99*, 103001.
- (32) Madsen, C. B.; Madsen, L. B.; Viftrup, S. S.; Johansson, M. P.; Poulsen, T. B.; Holmegaard, L.; Kumarappan, V.; Jørgensen, K. A.; Stapelfeldt, H. *Phys. Rev. Lett.* **2009**, *102*, 073007.
- (33) Madsen, C. B.; Madsen, L. B.; Viftrup, S. S.; Johansson, M. P.; Poulsen, T. B.; Holmegaard, L.; Kumarappan, V.; Jørgensen, K. A.; Stapelfeldt, H. *J. Chem. Phys.* **2009**, *130*, 234310.
- (34) Townsend, D.; Sussman, B. J.; Stolow, A. *J. Phys. Chem. A* **2011**, *115*, 357–373.
- (35) Lin, J.; Beratan, D. N. *J. Phys. Chem. A* **2004**, *108*, 5655–5661.
- (36) Moreno-García, P.; Gulcur, M.; Manrique, D. Z.; Pope, T.; Hong, W.; Kaliginedi, V.; Huang, C.; Batsanov, A. S.; Bryce, M. R.; Lambert, C.; Wandlowski, T. *J. Am. Chem. Soc.* **2013**, *135*, 12228–12240.
- (37) Waldron, D.; Haney, P.; Larade, B.; MacDonald, A.; Guo, H. *Phys. Rev. Lett.* **2006**, *96*, 166804.
- (38) Hansen, J. L.; Nielsen, J. H.; Madsen, C. B.; Lindhardt, A. T.; Johansson, M. P.; Skrydstrup, T.; Madsen, L. B.; Stapelfeldt, H. *J. Chem. Phys.* **2012**, *136*, 204310.
- (39) Coudert, L. H.; Pacios, L. F.; Ortigoso, J. *Phys. Rev. Lett.* **2011**, *107*, 113004.
- (40) Ashwell, B. A.; Ramakrishna, S.; Seideman, T. *J. Chem. Phys.* **2013**, *138*, 044310.
- (41) Zhao, Y.; Truhlar, D. G. *Theor. Chem. Acc.* **2007**, *120*, 215–241.
- (42) Weigend, F.; Ahlrichs, R. *Phys. Chem. Chem. Phys.* **2005**, *7*, 3297–3305.
- (43) Shao, Y.; et al. *Phys. Chem. Chem. Phys.* **2006**, *8*, 3172.
- (44) Seideman, T. *Phys. Rev. Lett.* **1999**, *83*, 4971–4974.
- (45) Seideman, T.; Hamilton, E. *Adv. At., Mol., Opt. Phys.* **2006**, *52*, 289–329.
- (46) Parker, S. M.; Ratner, M. A.; Seideman, T. *J. Chem. Phys.* **2011**, *135*, 224301.
- (47) Hankin, S.; Villeneuve, D.; Corkum, P.; Rayner, D. *Phys. Rev. Lett.* **2000**, *84*, 5082–5085.
- (48) Yatsushashi, T.; Obayashi, T.; Tanaka, M.; Murakami, M.; Nakashima, N. *J. Phys. Chem. A* **2006**, *110*, 7763–7771.
- (49) Grandbois, M. *Science* **1999**, *283*, 1727–1730.
- (50) Williams, P. D.; Reuter, M. G. *J. Phys. Chem. C* **2013**, *117*, 5937–5942.